

B–H $\cdots\pi$ Interaction: A New Type of Nonclassical Hydrogen Bonding

Xiaolei Zhang,^{†,§} Huimin Dai,^{†,§} Hong Yan,^{*,†} Wenli Zou,[‡] and Dieter Cremer^{*,‡}

[†]State Key Laboratory of Coordination Chemistry, School of Chemistry and Chemical Engineering, Nanjing University, Nanjing, Jiangsu 210093, China

[‡]Computational and Theoretical Chemistry Group (CATCO), Department of Chemistry, Southern Methodist University, Dallas, Texas 75275-0314, United States

S Supporting Information

ABSTRACT: For the first time, nonclassical hydrogen (H)-bonding involving a B–H $\cdots\pi$ interaction is described utilizing both quantum chemical predictions and experimental realization. In the gas phase, a B–H $\cdots\pi$ H-bond is observed in either B₂H₆ \cdots benzene ($\Delta E = -5.07$ kcal/mol) or carborane \cdots benzene ($\Delta E = -3.94$ kcal/mol) complex at reduced temperatures. Ir-dimercapto-carborane complexes [Cp*Ir(S₂C₂B₁₀H₁₀)] are designed to react with phosphines PR₃ (R = C₆H₄X, X = H, F, OMe) to give [Cp*Ir(PR₃)S₂C₂B₁₀H₁₀] for an investigation of B–H $\cdots\pi$ interactions at ambient temperatures. X-ray diffraction studies reveal that the interaction between the carborane BH bonds and the phosphine aryl substituents involves a BH $\cdots\pi$ H-bond (H $\cdots\pi$ distance: 2.40–2.76 Å). ¹H NMR experiments reveal that B–H $\cdots\pi$ interactions exist in solution according to measured ¹H{¹¹B} signals at ambient temperatures in the range 0.0 ≤ δ ≤ 0.3 ppm. These are high-field shifted by more than 1.5 ppm relative to the ¹H{¹¹B} signals obtained for the PMe₃ analog without B–H $\cdots\pi$ bonding. Quantum chemical calculations suggest that the interaction is electrostatic and the local (B)H $\cdots\pi$ ring stretching force constant is as large as the H-bond stretching force constant in the water dimer.

The noncovalent interaction between an X–H bond and an aromatic ring has been described as nonclassical (weak) hydrogen bond (H-bond, $\Delta E < 5$ kcal/mol) of the type X–H $\cdots\pi$ (X = C, N, O), which is of considerable importance in structural biology.¹ C–H $\cdots\pi$,² N–H $\cdots\pi$,³ and O–H $\cdots\pi$ ⁴ interactions have been documented utilizing both experimental and computational means for benzene-haloalkane, benzene-ammonia, and benzene-water complexes. More recently, carborane has been exploited for a new drug design^{5a} based on the exploitation of a proton-hydride (H δ^- \cdots H δ^+) dihydrogen bond^{5b} ($\Delta E = \sim -5$ kcal/mol) between the B–H bond in carborane and the proton donor in biomolecules. However, the potential interaction between a B–H bond and the π face of an aromatic moiety in the sense of a B–H $\cdots\pi$ interaction has not been reported so far.

The strength of the X–H $\cdots\pi$ interaction increases with increasing polarity of the X–H bond where X has to be more electronegative than H. In view of the electropositive character of boron ($\chi(\text{B}) = 2.04$ vs $\chi(\text{H}) = 2.20$),^{5c} B–H $\cdots\pi$ interactions should be repulsive rather than attractive. This is in line with the fact that ω B97X-D⁶ calculations with a basis set including diffuse

functions (6-31++G(d,p))⁷ describe the BH₃ \cdots C₆H₆ complex **A1** (Figure 1) as a second-order transition state of low stability

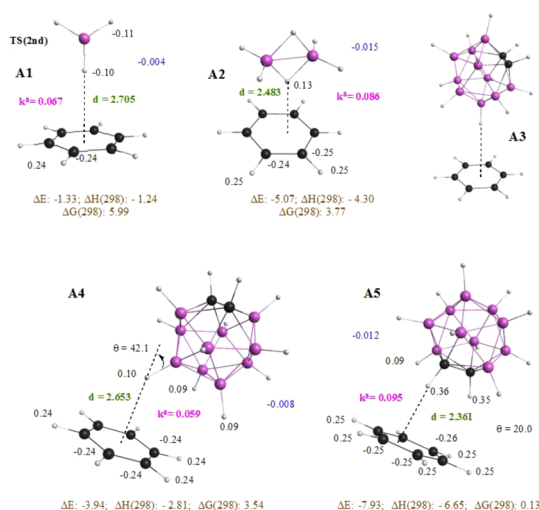


Figure 1. Calculated properties of reference molecules **A1**–**A5**. Blue numbers: total charge transfer from benzene to the borane in electrons; numbers close to atom balls: NBO charges of a given atom in electrons. **A1** is a second-order transition state (TS(2nd)); ω B97X-D/6-31++G(d,p) calculations.

($\Delta E = -1.33$ kcal/mol). **A1** rearranges to a BH₃-benzene complex in which the two molecules are located in parallel planes and the B atom is above the C atom so that the attraction between the two oppositely charged atoms is maximal. Other weakly stabilized BH₃ \cdots C₆H₆ forms involve the in-plane approach between the H(B) and H(C) atoms (H δ^- \cdots H δ^+ dihydrogen interactions) as they are known for borazane.⁷

To increase the strength of the B–H $\cdots\pi$ interactions, an inverse polarity of the B–H bond is required, which is realized in the B₂H₆ \cdots benzene complex **A2** (Figure 1). Two-electron-three-center (2e-3c) bonding leads to a positively charged μ^2 -H atom (0.13 e), which is attracted by the π -density of the benzene and accepts from the latter 15 me (millielectron) negative charge. The shortest distance (d) between benzene ring and the H atom is 2.48 Å, and the binding energy $\Delta E = -5.07$ kcal/mol similar to that of the water dimer (-5.0 kcal/mol),⁸ which is in line with the local (B)H $\cdots\pi$ (benzene) stretching force constant k^d of 0.086

Received: February 3, 2016

Published: February 24, 2016

mdyn/Å (water dimer: 0.087 mdyn/Å).⁸ Since the local stretching force constant provides an absolute measure of the bond strength of an individual bond,⁹ can be determined from measured frequencies as in the case of the water dimer,⁸ and is not contaminated by mode–mode coupling, its value in combination with the calculated ΔE suggests attractive B–H $\cdots\pi$ interactions in the sense of a nonclassical H-bond. However, complex **A2** can only be observed at low temperature because of an entropy penalty and a free energy value $\Delta G(298)$ of 3.77 kcal/mol (Figure 1).

Another class of molecules with positively charged H(B) atoms are carboranes.¹⁰ Carboranes form stabilizing B–H $\cdots\pi$ interactions with benzene in a different way than shown for **A3** (Figure 1; initial T-structure based on the attraction of one positively charged H(B) atom and the π -density of benzene as found for the T-structure of the benzene dimer).¹¹ Complex **A3** stabilizes by tilting (tilted T-structure) and augmenting the primary B–H $\cdots\pi$ interaction by two secondary B–H $\cdots\pi$ electrostatic attractions (**A4**, Figure 1). Complex **A4** is characterized by a binding energy ΔE of -3.94 kcal/mol, a charge transfer of just 8 me from benzene to *o*-carborane, a (B)H $\cdots\pi$ local stretching force constant of 0.059 mdyn/Å, and a distance d of 2.653 Å, indicating a weaker B–H $\cdots\pi$ interaction than that in **A2**. If complexation involves the more polar CH bonds of *o*-carborane, the corresponding parameters ($\Delta E = -7.93$ kcal/mol, charge transfer: 12 me; $k^a = 0.095$ mdyn/Å, $d = 2.361$ Å) describe a much stronger C_{carb}–H $\cdots\pi$ interaction (Figure 1) (Note that similar C_{carb}–H $\cdots\pi$ H-bonds have been described in carborane supramolecular chemistry.¹²) Again, vibrational and entropic penalties render both complexes **A4** and **A5** unstable at room temperature ($\Delta G(\mathbf{A4}, 298) = 3.54$, $\Delta G(\mathbf{A5}, 298) = 0.13$ kcal/mol, Figure 1). According to the literature, B–H $\cdots\pi$ interactions should also exist in carborane inclusion complexes,¹³ but have not been recognized so far. Therefore, we suppose that the B–H $\cdots\pi$ nonclassical H-bond might be stabilized at room temperature by incorporating it in a suitable template as indicated in Figure 2.

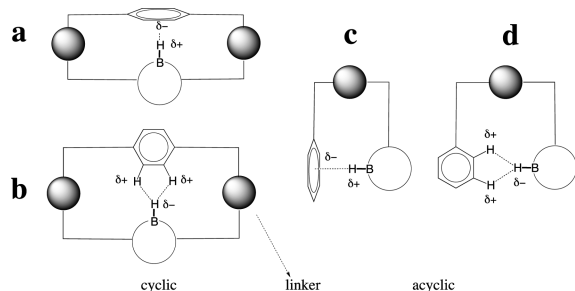


Figure 2. Possible molecular templates to enforce intramolecular interactions involving the BH bond and leading to either B–H $\cdots\pi$ H-bonding (a and c) or to H δ^- \cdots H δ^+ interactions (b and d) as in solid borazane.

Template **a** or **b** (Figure 2) with its cyclic topology may enforce B–H \cdots aryl interactions, provided the framework of the template guarantees sufficient rotational flexibility for the C₆H₄ group so that either B–H $\cdots\pi$ H-bonding (**a**) or H δ^- \cdots H δ^+ interactions⁷ (**b**) become possible. Synthetically demanding is also the acyclic template **c** or **d** where, as a result of a suitable steric arrangement of the linker group, the intramolecular carborane-aryl interactions are realized. In this work, the second possibility was pursued starting from half-sandwich 16e Ir

dithiolene complexes [Cp*Ir(S₂C₂B₁₀H₁₀)] (**A6**, Figure 3). Both **B** and **C** (corresponding to a boron- or carbon-sulfur linking of *o*-

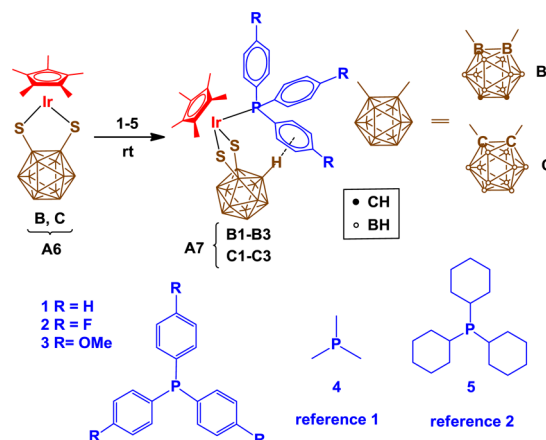


Figure 3. Formation of Ir-phosphine complexes **A7** from **A6**. Phosphines 1–5 were reacted with **A6** (**B** and **C**) at room temperature leading for 1–4 to two sets of 18e complexes (**A7**) containing the B–H $\cdots\pi$ H-bond in **B1**–**B3** and **C1**–**C3**.

carborane) were used thus providing different chemical environments for the BH vertexes in the two complexes. Reactions of **A6** with phosphines 1–3 should generate the 18e complexes **A7** (Figure 3), which requires that the phosphine ligand with the three aryl substituents can enter the coordination sphere of the metal center. This can be accomplished by shifting of the Cp* ligand to the back side of the Ir atom, back-folding of the dimercapto-carboranyl ligand, and increasing the pyramidalization of the phosphine.

Tests aimed at exploring the limitations of the reaction **A6** + PR₃ → **A7** were performed with trimethylphosphine and tricyclohexyl phosphine. For PMe₃, stable 18e complexes **B4** and **C4** were readily formed, whereas for P(cyclo-C₆H₁₁)₃ (**5**), a stable complex could not be formed even when varying the reaction conditions. Obviously, steric crowding introduced by the phosphine ligand hinders the extension of the Ir coordination sphere in the latter case. Nevertheless, it was surprising that all phenyl-substituted phosphines yielded stable **A7** derivatives **B1**–**B3** containing a B–S(Ir) linkage and **C1**–**C3** containing a C–S(Ir) linkage at room temperature, in which one B–H bond points toward one aryl ring of the phosphine to form a B–H $\cdots\pi$ H-bond. The different *p*-phenyl substituents (i.e., R = H, F, OMe) were introduced to vary the π -density for an investigation of its influence on the B–H $\cdots\pi$ interaction. Note that complex [Cp*Ir(PMe₃)(1,2-S₂C₂B₁₀H₁₀)]¹⁴ (**C4**) has been reported previously, whereas the seven complexes **B1**–**B4** and **C1**–**C3** are investigated for the first time.

The structure determination of these complexes was performed by a three-pronged approach based on X-ray diffraction analysis (solid state), NMR spectroscopy (solution), and quantum chemical calculations (gas phase). In Figure 4, the X-ray structure of **B1** is compared with the corresponding gas-phase structure. Steric repulsion is lowered by (i) a distorted propeller conformation of the phenyl groups; (ii) shifting of Cp* ligand; (iii) the envelope puckering of the five-membered ring Ir₁S₂X₂ (X = B, C) as measured by the folding angle α ; and (iv) a single phenyl-carborane attraction (B13–H $\cdots\pi$, Figure 4). The attraction is of the B–H $\cdots\pi$ type rather than the H δ^- \cdots H δ^+ type (Figure 2) and strongly determines the configuration of **B1** and

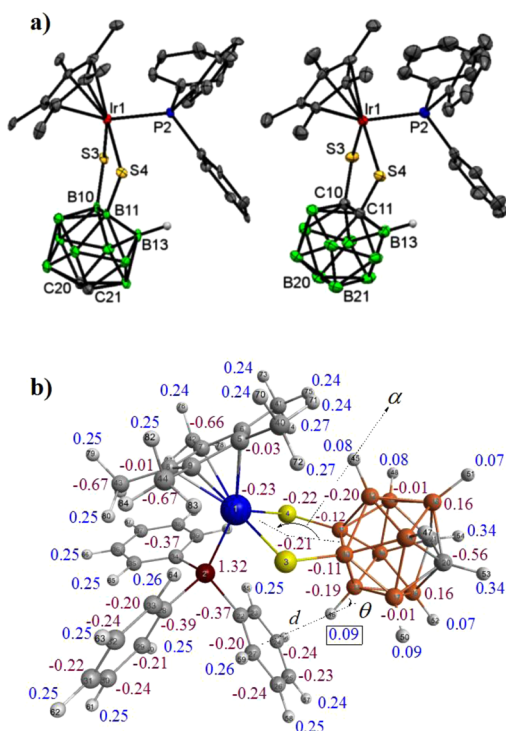


Figure 4. (a) X-ray structures of B1 (left) and C1 (right). (b) Calculated geometry of B1 shown together with calculated NBO charges;¹⁵ (ω B97X-D/def2-TZVPP/6-31++G(d,p) calculations).

the five other complexes B2, B3, C1–C3. Table 1 summarizes some structural parameters, which reveal that for B1–B3 and

Table 1. Structural Parameters of Complexes B1–B3 and C1–C3 Describing the Steric Interactions between the Ligands in A7^a

entry	α /(deg)		Ir–P/Å		d/Å		θ /(deg)		Charge(e)
	exp.	theo.	exp.	theo.	exp.	theo.	exp.	theo.	
B1	159	157.7	2.27	2.301	2.48	2.443	17	22.0	0.09
B2	157	157.5	2.27	2.297	2.76	2.432	23	22.0	0.09
B3	157	157.7	2.27	2.305	2.72	2.422	22	20.9	0.09
C1	156	156.6	2.28	2.318	2.65	2.368	24	10.9	0.05
C2	159	156.3	2.28	2.315	2.40	2.365	12	10.7	0.06
C3	158	156.7	2.29	2.322	2.48	2.346	11	9.2	0.06

^aParameters are explained in Figure 4b. Computed values theo. according to ω B97X-D/def2-TZVPP/6-31++G(d,p) calculations.

C1–C3, the shortest B–H $\cdots\pi$ distance is 2.40 ± 0.05 Å, and the positioning of the B–H bond above the phenyl ring is almost perpendicular (deviation angle θ : 9 – 22° , Table 1).

Next, we tried to verify the existence of the B–H $\cdots\pi$ H-bond in solution by ^1H NMR. Complexes A7 were immediately formed in solution as verified by new signals of BH and Cp* in the $^1\text{H}\{^{11}\text{B}\}$ NMR titration experiments (Figure S11). One BH resonance was observed at high field (i.e., $\delta \sim 0.3$ ppm for B1–B3 and ~ 0.0 ppm for C1–C3) at room temperature, which is distinct from the other BH signals appearing in the range of 1.4–3.0 ppm (Figures 5 and S11). This is in line with a shielding of the proton due to the ring current of the nearby phenyl ring. By

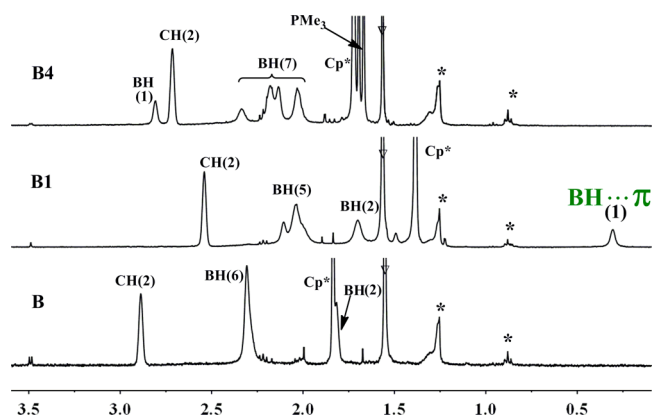


Figure 5. Expanded $^1\text{H}\{^{11}\text{B}\}$ NMR spectra of B, B1, B4 in CDCl_3 at room temperature with assignments. The number in bracket represents the number of hydrogen atoms. B–H $\cdots\pi$ proton signals in B1 is shown in the high field in green. (*: grease, ∇ : water). Note: For the similar spectra of C, C1, C4 as well as the complete set of spectra, see SI-Figure S12.

comparison, the reference complexes B4 and C4, in which a B–H $\cdots\pi$ interaction can not exist, as well as the starting complexes B and C show only the typical B–H resonances between 1.4 and 3.0 ppm for the carboranyl units (Figures 5 and S12). These results confirm the formation of the B–H $\cdots\pi$ H-bond, which stabilizes complexes A7 (B1–B3, C1–C3) in solution. Note that the high-field shifting of the BH signals could also be observed in an *o*-carborane inclusion complex^{13a} in which it was also caused by B–H $\cdots\pi$ interactions, however, the B–H $\cdots\pi$ H-bond could not be unambiguously confirmed by the X-ray diffraction analysis owing to a structural disorder of the carboranyl unit.

Our experimental studies confirm the existence of the B–H $\cdots\pi$ interactions in both solid state and in solution. However, the electronic trends caused by different BH vertexes in the carborane and different *p*-phenyl substituents of the phosphine ligand were disguised largely by crystal packing effects in the solid state. The situation becomes more complicated by the fact that B3 and C2 contain two molecules in one unit cell. Hence, quantum chemical calculations were needed for complexes A7 to unravel these effects. The calculated natural bond order (NBO) charges¹⁵ of H(B) vary between 0.05 (C structures) and 0.09 e at a *d*-value ≤ 2.44 Å (B structures, Table 1), which indicates a somewhat stronger attraction than in the reference molecule A4 (0.10 e, *d* = 2.65 Å). This is confirmed by the calculated B–H $\cdots\pi$ local stretching force constants (Table 2 and Figure 1) based on the Konkoli–Cremer mass-decoupled local vibrational modes.^{9a} It has been shown that local stretching constants k^d are proportional to the intrinsic strength of a bond, and their analysis can be facilitated by deriving a relative bond strength order (BSO) *n* derived from k^d by using suitable reference bonds as, for example, the BH bond of BH₃, the FH bond, and the H \cdots F bond in FHF[−].^{9c,16} In Table 2, the local mode properties of the complexes B1–B3 and C1–C3 are listed. They reveal that the intramolecular B–H $\cdots\pi$ interactions are stronger than in the complex A4. Also, distances *d* are shorter and k^d constants are larger, where the latter lead to BSO values of 0.347–0.364 (Table 2, A4: 0.247; A5 with its C–H $\cdots\pi$ interaction: 0.309).

In the series C1–C3, an increase in the π -density of the aryl ring due to a stronger π -donor substituent (H, F, OCH₃) should lead to an increase of the strength of the B–H $\cdots\pi$ interaction, which is observed (Table 2), whereas for the series B1–B3 the BSO (H $\cdots\pi$) value is stronger for B3 but weakest for B2. There is

Table 2. Distances (d), Local Stretching Force Constants and Frequencies (k^a and ω^a), and BSO Values n of the B–H $\cdots\pi$ Nonclassical H-Bonds^a

Complex	Local mode	$d(\text{H}\cdots\pi)$ Å	$k^a(d)$ mdyn/Å	$\omega^a(d)$ cm ⁻¹	$n(\text{H}\cdots\pi)$
A2	(B-)H $\cdots\pi$	2.483	0.086	382	0.300
A4	(B-)H $\cdots\pi$	2.653	0.059	276	0.247
A5	(C-)H $\cdots\pi$	2.361	0.095	402	0.309
B1	(B-)H $\cdots\pi$	2.443	0.143	495	0.348
B2	(B-)H $\cdots\pi$	2.432	0.142	492	0.347
B3	(B-)H $\cdots\pi$	2.422	0.159	520	0.359
C1	(B-)H $\cdots\pi$	2.368	0.158	519	0.358
C2	(B-)H $\cdots\pi$	2.365	0.161	524	0.360
C3	(B-)H $\cdots\pi$	2.346	0.167	534	0.364

^aThe distance d for (B)H $\cdots\pi$ (C₆) gives the shortest distance to the aryl ring plane as defined in Figures 1 and 4b; (ω B97X-D/def2-TZVPP/6-31++G(d,p) calculations).

no indication for a covalent interaction introduced by a charge transfer from the aryl ring into the $\sigma^*(\text{BH})$ antibonding orbital. The latter would lead to B–H bond lengthening contrary to the calculated B–H values in the series **B1**, **B2**, **B3** (1.180, 1.180, 1.179 Å) or **C1**, **C2**, **C3** (1.172, 1.173, 1.172 Å). Energy density studies according to the Cremer–Kraka criterion^{17a,b} suggest electrostatic interactions, which are significantly increased by space confinement similar to what is found for the bay C–H bonds of phenanthrene.^{17c} We note that the B–H $\cdots\pi$ interaction is slightly stronger than the H-bond in the water dimer because the mechanism of bonding is different in the two cases. H-bonding in the water dimer includes some covalent character due to a charge transfer, which is reflected by a lengthening of the O–H donor bond.⁸

In conclusion, B–H $\cdots\pi$ interaction has been documented and analyzed for the Ir dithiolenephosphine complexes [Cp*Ir(PR₃)₂S₂C₂B₁₀H₁₀] (**A7**: **B1–B3**, **C1–C3**) employing X-ray diffraction, NMR spectroscopy, and quantum chemical calculations. In the experimental observation for the 18e Ir complexes **A7**, the B–H $\cdots\pi$ interactions are stronger than in the reference complexes **A2** and **A4**, as is documented by the local B–H $\cdots\pi$ stretching force constants and the corresponding BSO values (**A7**: 0.347–0.364; **A2**: 0.300; **A4**: 0.242). Quantum chemical calculations reveal that the B–H $\cdots\pi$ distances d (2.346–2.443 Å) are shorter than the sum of van der Waals radii of H and C (~3.0 Å), and in all cases, B–H $\cdots\pi$ H-bonding is electrostatic in nature.

■ ASSOCIATED CONTENT

📄 Supporting Information

Experimental details and data. The Supporting Information is available free of charge on the ACS Publications website at DOI: 10.1021/jacs.6b01249.

■ AUTHOR INFORMATION

Corresponding Authors

*hyan1965@nju.edu.cn

*dcremer@smu.edu

Author Contributions

[§]These authors contributed equally.

Notes

The authors declare no competing financial interest.

■ ACKNOWLEDGMENTS

At Nanjing, this work was supported by the National Basic Research Program of China (2013CB922101) and NSFC (21271102, 21472086 and 21531004). At SMU, the work was supported by the NSF (Grants CHE 1152357 and 1464906). We thank the High Performance Computing Centers of SMU and Nanjing University for providing computational resources.

■ REFERENCES

- (a) Meyer, E. A.; Castellano, R. K.; Diederich, F. *Angew. Chem., Int. Ed.* **2003**, *42*, 1210. (b) Takahashi, O.; Kohno, Y.; Nishio, M. *Chem. Rev.* **2010**, *110*, 6049.
- (a) Lopez, J. C.; Caminati, W. J.; Alonso, L. *Angew. Chem., Int. Ed.* **2006**, *45*, 290. (b) Tsuzuki, S.; Honda, K.; Uchimaru, T.; Mikami, M.; Tanabe, K. *J. Phys. Chem. A* **2002**, *106*, 4423.
- (a) Rodham, D. A.; Suzuki, S.; Suenram, R. D.; Lovas, F. J.; Dasgupta, S.; Goddard, W. A., III; Blake, G. A. *Nature* **1993**, *362*, 735. (b) Vaupel, S.; Brutschy, B.; Tarakeswar, P.; Kim, K. S. *J. Am. Chem. Soc.* **2006**, *128*, 5416.
- (a) Suzuki, S.; Green, P. G.; Bumgarner, R. E.; Dasgupta, S.; Goddard, W. A., III; Blake, G. A. *Science* **1992**, *257*, 942. (b) Pribble, R. N.; Zwier, T. S. *Science* **1994**, *265*, 75.
- (a) Lee, M. W., Jr.; Sevryugina, Y. V.; Khan, A.; Ye, S. Q. *J. Med. Chem.* **2012**, *55*, 7290. (b) Fanfrlík, J.; Lepšík, M.; Horinek, D.; Havlas, Z.; Hobza, P. *ChemPhysChem* **2006**, *7*, 1100. (c) Haynes, W. M.; Lide, D. R.; Bruno, T. J. *CRC Handbook of Chemistry and Physics*; CRC Press: Boca Raton, FL, 2013.
- (a) Chai, J. D.; Head-Gordon, M. *Phys. Chem. Chem. Phys.* **2008**, *10*, 6615. (b) Chai, J. D.; Head-Gordon, M. *J. Chem. Phys.* **2008**, *128*, 084106.
- Klooster, W. T.; Koetzle, T. F.; Siegbahn, P. E.; Richardson, T. B.; Crabtree, R. H. *J. Am. Chem. Soc.* **1999**, *121*, 6337.
- Kalescky, R.; Zou, W.; Kraka, E.; Cremer, D. *Chem. Phys. Lett.* **2012**, *554*, 243.
- (a) Kraka, E.; Larsson, J. A.; Cremer, D. in *Computational IR Spectroscopy*, Grunenberg, J., Ed.; Wiley: New York, 2010; pp 105–149. (b) Kalescky, R.; Kraka, E.; Cremer, D. *J. Phys. Chem. A* **2013**, *117*, 8981. (c) Cremer, D.; Larsson, J. A.; Kraka, E. *Theoretical and Computational Chemistry, Theoretical Organic Chemistry*, Parkanyi, C., Ed.; Elsevier: Amsterdam, 1998, Vol 5, p 259.
- (a) Hosmane, N. S. *Boron Science: New Technologies and Applications*; CRC Press: Boca Raton, FL, 2011. (b) Grimes, R. N. *Carboranes*, 2nd ed.; Elsevier: Amsterdam, 2011.
- (a) Grafenstein, J.; Cremer, D. *J. Chem. Phys.* **2009**, *130*, 124105.
- (a) Issa, F.; Kassiou, M.; Rendina, L. M. *Chem. Rev.* **2011**, *111*, 5701. (b) Fox, M. A.; Hughes, A. K. *Coord. Chem. Rev.* **2004**, *248*, 457.
- (a) Kusukawa, T.; Fujita, M. *J. Am. Chem. Soc.* **2002**, *124*, 13576. (b) Raston, C. L.; Cave, G. W. V. *Chem. - Eur. J.* **2004**, *10*, 279.
- Bae, J. Y.; Park, Y. I.; Ko, J.; Park, K. I.; Cho, S. I.; Kang, S. O. *Inorg. Chim. Acta* **1999**, *289*, 141.
- Weinhold, F.; Landis, C. R. *Valency and Bonding: A Natural Bond Orbital Donor-Acceptor Perspective*; Cambridge University Press, Cambridge, U.K., 2003.
- Freindorf, M.; Kraka, E.; Cremer, D. *Int. J. Quantum Chem.* **2012**, *112*, 3174.
- (a) Cremer, D.; Kraka, E. *Angew. Chem., Int. Ed. Engl.* **1984**, *23*, 627. (b) Cremer, D.; Kraka, E. *Croat. Chem. Acta* **1984**, *57*, 1259. (c) Kalescky, R.; Kraka, E.; Cremer, D. *J. Phys. Chem. A* **2014**, *118*, 223.